

Causal Inference for Heritable Phenotypic Risk Factors Using Heterogeneous Genetic Instruments

Jingshu Wang^{*1}, Qingyuan Zhao², Jack Bowden³, Gilbran Hemani⁴, George Davey Smith⁴, Dylan S. Small⁵, and Nancy R. Zhang⁵

¹The University of Chicago

²University of Cambridge

³The University of Exeter

⁴University of Bristol

⁵University of Pennsylvania

Abstract

Over a decade of genome-wide association studies have led to the finding that significant genetic associations tend to be spread across the genome for complex traits, leading to the recent proposal of an "omnigenic" model where almost all genes contribute to every complex trait. Such an omnigenic phenomenon complicates Mendelian Randomization studies, where natural genetic variations are used as instruments to infer the causal effect of heritable risk factors. We reexamine the assumptions of existing Mendelian Randomization methods and show how they need to be revised to allow for pervasive pleiotropy and heterogeneous effect sizes. We propose a comprehensive framework GRAPPLE (Genome-wide mR Analysis under Pervasive PLEiotropy) to analyze the causal effect of a target risk factor with heterogeneous genetic instruments and identify possible pleiotropic patterns from data. By using summary statistics from genome-wide association studies, GRAPPLE can efficiently use both strong and weak genetic instruments, detect the existence of multiple pleiotropic pathways, adjust for confounding risk factors, and determine the causal direction. With GRAPPLE, we analyze the effect of blood lipids, body mass index, and systolic blood pressure on 25 disease outcomes, gaining new information on their causal relationships and the potential pleiotropic pathways.

1 Introduction

Understanding the pathogenic mechanism of common diseases is a fundamental goal in clinical research. As randomized controlled experiments are not always possible, researchers are looking towards Mendelian Randomization (MR) as an alternative method for probing the causal mechanisms of common diseases [16]. MR uses inherited genetic variation as "instrumental variables" to interrogate the causal effect of heritable risk factor(s) on the disease of interest. The basic idea is that at these variant loci, the inherited alleles are randomly drawn according to Mendel's laws, and thus are

*jingshuw@uchicago.edu

independent from non-heritable confounding variables which may obfuscate causal estimation [43]. With the accumulation of data from genome-wide association studies (GWAS), there is increasing interest in MR approaches, especially approaches that only rely on the GWAS summary statistics that are readily available in the public domain [17, 43].

How well Mendelian Randomization works depends on how well the genetic variant loci used as instruments abide by the rules of instrumental variables (IV). These rules dictate that, if the genetic loci has an effect on the disease outcome, it should be only through pathways mediated by the risk factor of interest. This rule, termed exclusion restriction, is often violated as we now know there is widespread horizontal pleiotropy, defined as cases where the genetic variant influences the risk factor and the disease outcome by independent pathways. There has been much recent attention on this issue [10, 4, 5, 22, 48, 56, 39, 11, 3, 34, 40], yet our understanding is far from complete. Current methods rely on different assumptions on the pattern of pleiotropy, while improper assumptions may lead to biased estimation of the true causal effects. What assumptions on pleiotropy and genetic effects would be suitable? Would it be possible to learn the degree of pleiotropy from the data? Could we perform model diagnosis utilizing only GWAS summary statistics?

The pleiotropy issue that muddle Mendelian Randomization studies is, in a large part, due to the fact that complex traits are highly polygenic [54, 30, 42, 46, 34]. Accumulating evidence from GWAS studies indicate that all complex diseases share a single "omnigenic" architecture [29, 6] where a few are "core" genes while almost all genes are peripherally involved and can exert non-zero effects on the disease through pathways that are unrelated to the risk factor of interest. Thus, not only do we expect pleiotropy to be a pervasive issue across all genetic variants, for any given disease or complex risk factor, it can also be associated with a large number of SNPs. Many existing MR methods rely on the assumption that pleiotropic effects sparsely involve only a few SNPs or that there is only one pleiotropic pathway, which directly counters these recent insights. Methods that don't assume sparsity requires that the pleiotropic effects cancel each other across SNPs, which is rather optimistic. Armed with these assumptions, most existing methods also utilize only the few SNPs that have the strongest association with the risk factor as instruments, ignoring the SNPs that are weakly associated. In this work, we will show that weakly associated SNPs are also informative, and that a model combining weak and strong SNPs would not harm MR while increasing its accuracy and stability in some scenarios.

We propose a comprehensive statistical framework for causal effect estimation when pleiotropy is pervasive across the genome. The framework, called GRAPPLE (Genome-wide mR Analysis under Pervasive PLEiotropy) facilitates interactive identification of pleiotropic pathways and the incorporation of all SNPs associated with the risk factor into the analysis. GRAPPLE builds on the statistical framework MR-RAPS [54] to allow the detection of the existence of multiple pleiotropic pathways as well as the discrimination of the direction of causality. Using GRAPPLE, we further address how to jointly estimate the effects of multiple risk factors, as well as how to integrate cohorts with overlapping samples, both common challenges faced by current studies. The estimation accuracy of GRAPPLE is examined through validations involving real studies.

GRAPPLE is applied to a screening of the causal effects of 5 risk factors (three plasma lipid traits, body mass index, and systolic blood pressure) on 25 common diseases. Although there has been many causal effect screens for these risk factors and diseases, the combined analysis enabled by GRAPPLE brings forth new insights on the pleiotropic landscape across diseases and, thus, an improved understanding of the causal estimates obtained. Specifically, we will reexamine the role of lipid traits on coronary artery disease and type-II diabetes, where the results from the multitude of MR studies [43, 28, 31] have been under heated debate.

2 Results

2.1 Model Overview

2.1.1 From the causal model to GWAS summary statistics

Our framework starts with a set of structural equations that jointly specify the generative model on the disease Y that relies on K candidate risk factors X_k , and all genetic variants $\mathbf{Z} = (Z_1, Z_2, \dots)$ (Figure 1a).

$$\begin{aligned} Y &= \mathbf{X}^T \boldsymbol{\beta} + f(\mathbf{U}, \mathbf{Z}, E_Y) \\ X_k &= g_k(\mathbf{U}, \mathbf{Z}, E_{X_k}), \quad k = 1, \dots, K \end{aligned} \quad (1)$$

where \mathbf{U} represents unknown non-heritable confounding factors and E_{X_k} and E_Y are random noise acting on X_k and Y respectively. The parameter of interest, $\boldsymbol{\beta}$, quantifies the causal effect of the vector of risk factors \mathbf{X} on Y . Due to Mendel’s law of inheritance, the genotypes \mathbf{Z} are independent of \mathbf{U}, E_Y, E_{X_k} . The function $f(\mathbf{U}, \mathbf{Z}, E_Y)$ represents the causal effects of unmeasured risk factors on Y , which can be heritable (contributed by \mathbf{Z}) or non-heritable (contributed by \mathbf{U}). The non-parametric functions $f(\cdot)$ and $g_k(\cdot)$ allow interactions among SNPs in \mathbf{Z} and variables $(\mathbf{U}, E_Y, E_{X_k})$ in their causal effects on \mathbf{X} and Y . Under this model, the exclusion restriction assumption is violated for a SNP j if Z_j has nonzero association with $f(\mathbf{U}, \mathbf{Z}, E_Y)$. This is the case, for example, when Z_j acts on Y through a pathway unrelated to X , or when Z_j is in linkage disequilibrium with such a loci.

Now consider the case where only GWAS summary statistics, i.e. the estimated marginal associations between each SNP j and the risk factors/disease traits, are available. Let Γ_j be the true association between SNP j and Y , and $\boldsymbol{\gamma}_j$ be the vector of true marginal associations between SNP j and \mathbf{X} . Later, we will denote their estimated values from GWAS summary statistics as $\hat{\Gamma}_j, \hat{\boldsymbol{\gamma}}_j$. Then, as shown in Methods, the model (1) results in the linear relationship

$$\Gamma_j = \boldsymbol{\gamma}_j^T \boldsymbol{\beta} + \alpha_j \quad (2)$$

This relationship holds even when the functions $f(\cdot)$ and $g(\cdot)$ in (1) are not linear. Here, α_j is the marginal association between Z_j and $f(\mathbf{U}, \mathbf{Z}, E_Y)$, representing the unknown pleiotropic effect of SNP j .

One can immediately see that identifying $\boldsymbol{\beta}$ is impossible without assumptions on α_j . The simplest assumption is that all instruments are valid and satisfy $\alpha_j = 0$ [16, 10]. However, this or more generally the assumption that α_j is sparse [5, 48] in selected SNPs, seem unlikely given recent GWAS findings of weakly associated SNPs spread across the genome for most traits. There is pervasive pleiotropy where almost all $\alpha_j \neq 0$ even when only strongly associated SNPs are selected, as core genes of the target risk factors are also “peripheral” for unmeasured risk factors. One assumption that allow pervasive pleiotropy is the “almost random effect” model [56, 40], where $\alpha_j \sim \mathcal{N}(0, \tau^2)$ is satisfied for most genetic instruments, indicating that the pleiotropic effects are mostly balanced out. However, if there are unmeasured main risk factors and a cluster of SNPs are associated with both the unmeasured risk factors and \mathbf{X} , the pleiotropic effects are unlikely to balance out as SNPs that share the same pleiotropic pathway will have the same direction of pleiotropy. Some MR methods aim to identify causal effects assuming that there is only one pleiotropic pathway [36, 34, 11, 39].

2.1.2 Identify multiple pleiotropic pathways and the direction of causality using the shape of a profile likelihood

The key idea underlying GRAPPLE is to detect multiple pleiotropic pathways by using the shape of the profile likelihood, and not just the location of its maximum, to probe the underlying causal

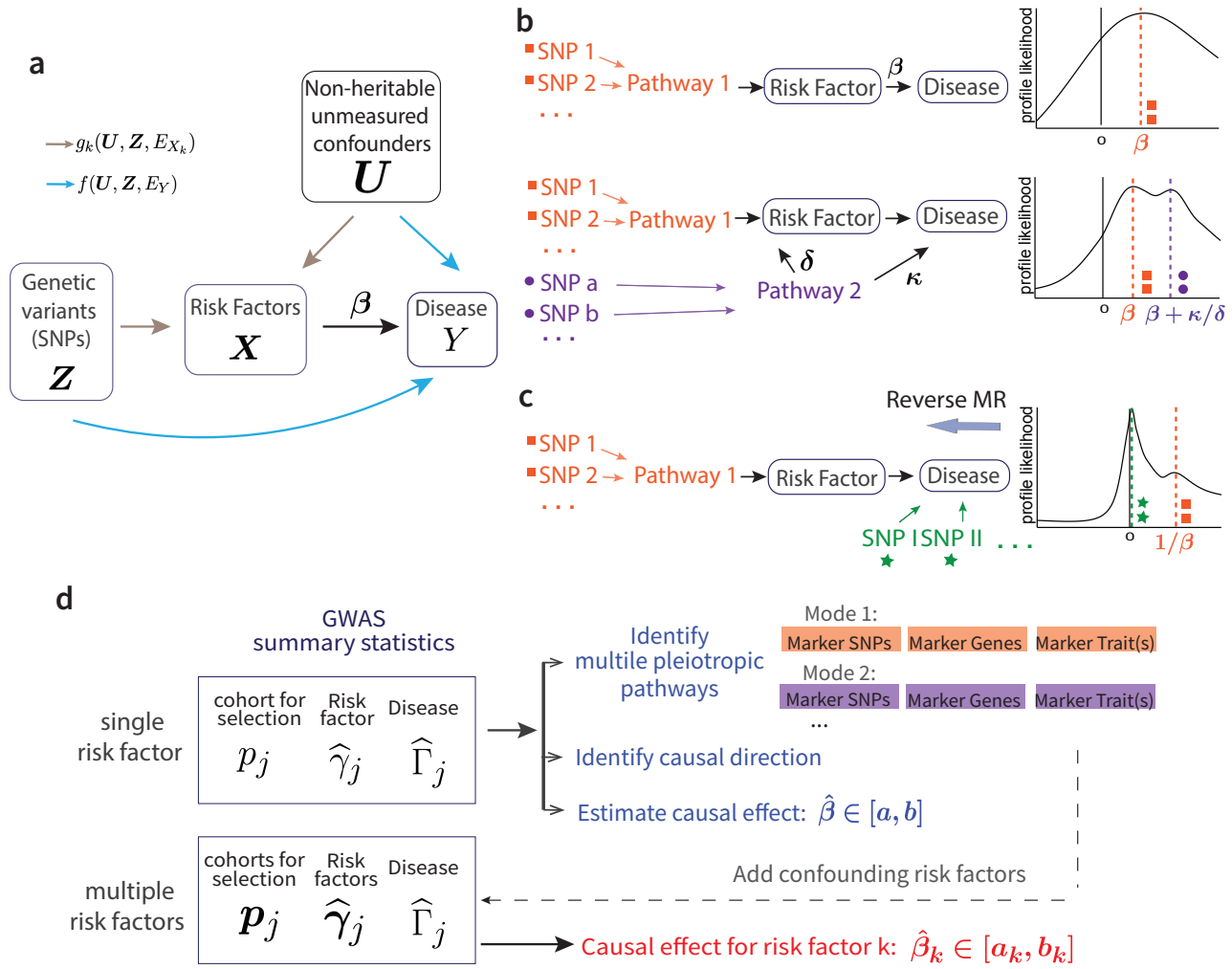


Figure 1: Model overview. **a**, The causal directed graph represented by structural equations (1). **b**, The existence of a pleiotropic pathway 2 (purple) can result in multiple modes of the profile likelihood. **c**, Multi-modality of the profile likelihood can reflect causal direction. **d**, The work-flow with GRAPPLE.

mechanism (Figure 1b). When $K = 1$, the GWAS summary statistics reduce to the scalar $\hat{\gamma}_j$ and $\hat{\Gamma}_j$, with their standard errors σ_{1j}^2 and σ_{2j}^2 . From the central limit theorem, the joint distribution of $(\hat{\gamma}_j, \hat{\Gamma}_j)$ approximately follows a multivariate normal distribution

$$\begin{pmatrix} \hat{\gamma}_j \\ \hat{\Gamma}_j \end{pmatrix} \sim \mathcal{N} \left(\begin{pmatrix} \gamma_j \\ \Gamma_j \end{pmatrix}, \begin{pmatrix} \sigma_{1j}^2 & \sigma_{1j}\sigma_{2j}\theta \\ \sigma_{1j}\sigma_{2j}\theta & \sigma_{2j}^2 \end{pmatrix} \right) \quad (3)$$

where θ is a shared sample correlation that can be estimated as $\hat{\theta}$ (see Methods).

Consider, first, the case where a second genetic pathway (Pathway 2) also contributes substantially to the disease, and where some of the loci that we include as instruments are also associated with Pathway 2 (Figure 1b). When there is no pleiotropy in the p selected independent genetic instruments, the robustified profile likelihood [56],

$$l(b) = - \sum_{i=j}^p \rho \left(\frac{\hat{\Gamma}_j - b\hat{\gamma}_j}{\sqrt{\sigma_{1j}^2 + b^2\sigma_{2j}^2 + 2b\hat{\theta}\sigma_{1j}\sigma_{2j}}} \right) \quad (4)$$

where $\rho(\cdot)$ is Tukey’s biweight loss would only have one mode near the true causal effect $b = \beta$ as for every instrument j there is $\Gamma_j = \beta\gamma_j$. However, under the existence of Pathway 2, SNPs that are associated with X only through Pathway 2 may contribute to a second mode in the profile likelihood at location $\beta + \kappa/\delta$, where κ and δ quantifies the causal effect of Pathway 2 on Y and its marginal association with X , respectively (Methods). By similar logic, multiple pleiotropic pathways result in multiple modes in the profile likelihood. Thus, GRAPPLE uses the presence of multiple modes in the profile likelihood to diagnose the presence of pleiotropy, and identifies the SNPs that contribute to these modes which can be informative for genes that act in these alternative pathways. Specifically, GRAPPLE outputs the marker SNPs, as well as the mapped genes and GWAS traits of each marker SNP (see Methods). To increase sensitivity, the profile likelihood for mode detection are robustified and ignores the small non-directional pleiotropic effects.

Now consider the question of whether X indeed causes Y , as our structural equation (1) presumes, or is it the reverse case of Y causing X . If it were the case that the direction of causality runs from Y to X , then an instrument is associated with X either through Y , or through other heritable risk factors of X unrelated to Y . In the latter case, a SNP j satisfies $\gamma_j \neq 0$ while $\Gamma_j = 0$, and would contribute to a mode at 0. In the former case, $\gamma_j = \beta\Gamma_j$ where β is the causal effect of Y on X , and these SNPs may contribute to a mode around $1/\beta$. This idea shares similarities with Bidirectional MR [47, 23]. Bidirectional MR is based on the assumptions that when MR is reversely performed, all selected instruments affect Y not through X , and filter out suspicious SNPs that may violate this assumption by checking their associations with X . Though it sometimes works, there is no guarantee that the filtering does not introduce bias. In GRAPPLE, we identify the direction by checking if there is a mode at 0 after switching the roles of X and Y , while tolerating the existence of another mode around $1/\hat{\beta}$.

2.1.3 Weak genetic instruments: A curse or a blessing?

Besides the assumption of no-horizontal-pleiotropy, for a SNPs to be a valid genetic instrument, it needs to have non-zero association with the risk factor of interest. In most MR pipelines, SNPs are selected as instruments only when their p-values are below 10^{-8} , which is required to guarantee a low family-wise error rate (FWER). Using such a stringent threshold also avoids weak instrument bias [13], where noise in the estimate $\hat{\gamma}_{jk}$ are too large to lead to bias in the estimate $\hat{\beta}$ of the causal effect. However, such a stringent selection threshold may result in very few, or even zero, instruments for under-powered GWAS. Further, when our goal is to jointly model the effects of multiple risk factors (the setting where X as a vector in GRAPPLE), it is unrealistic to assume that all instruments have strong effects on every risk factor. In addition, the highly polygenecity phenomenon of complex traits indicates that the number of weak instruments far outnumbers the number of strong instruments, and collectively, they may exert a positive effect on the estimation accuracy.

In GRAPPLE, we use a flexible p-value threshold, which can either as stringent as 10^{-8} or as mild as 10^{-2} , for instrument selection. Based on the framework of MR-RAPs [55], GRAPPLE can provide valid inference of $\hat{\beta}$ with both strong and weakly associated SNPs, under the “almost random effect” assumption of pleiotropy. This flexible p-value threshold is beneficial for several reasons. First, including moderate and weak instruments may increase power, especially for under-powered GWAS data where there are too few strongly associated SNPs. Second, MR for multiple risk factors are more accurate as including SNPs that do not have strong association with every risk factor is inevitable. Third, the modes of the profile likelihood that is used for identifying pleiotropic pathways are less affected by single outliers with a milder threshold than 10^{-8} . Lastly, comparing estimates across a series of p-value thresholds can show stability of our estimates and a more complete picture of the underlying pleiotropy.

2.1.4 The three-sample design to guard against instrument selection bias

Selecting instruments from GWAS summary statistics can also introduce bias, which is the “winner’s curse”. The magnitude of $\hat{\gamma}_{jk}$ will increase conditional on being selected and would bias the estimate β . When $K = 1$ that there is only one risk factor, the estimate will bias towards 0, but there is no guarantee of the direction of the bias when $K > 1$. Typically, it is believed that the selection bias is negligible when only the strongly associated SNPs are selected as instruments. The selection bias will be more severe with weak genetic instruments.

However, we find that instrument selection can introduce bias even when only genetic variants with genome-wide significant p-values ($\leq 10^{-8}$) are selected. Thus, unlike the usual two-sample GWAS summary statistics design which involves one GWAS data for the risk factor and one for the disease, in GRAPPLE we strongly advocate using a three-sample GWAS summary statistics design. To avoid the selection bias, selection of genetic instruments is done on another GWAS dataset for the risk factor, whose cohort has no overlapping samples with both the risk factor and disease cohorts. In addition, to ease calculation (see Methods), currently we only include independent SNPs in GRAPPLE and we use the LD clumping for SNP selection to obtain them [38]. The three-sample design will also avoid possible selection bias introduced during clumping.

Summarizing the above points, a complete diagram of the GRAPPLE workflow is shown in Figure 1d. A researcher may start with a single target risk factor of interest. The shape of the robustified profile likelihood provides information on possible pleiotropic pathways. When there is only one mode, the “almost random effect” assumption on the pleiotropic effects would likely to be reasonable and one can estimate the causal effect of the risk factor using MR-RAPS. Instead, if multiple modes are detected, then one may need to adjust for pleiotropic pathways. Unfortunately, this step can not be done automatically as summary statistics themselves do not provide enough information to distinguish a causal mode from a pleiotropic mode, and expert knowledge is needed. Researchers can use the marker SNP/gene/trait information that GRAPPLE provides to understand each mode, decide which confounding risk factors to adjust for, and collect extra GWAS data for them. Assuming that pleiotropic effects follow an “almost random effect” model after adjusting for the confounding risk factors, GRAPPLE can then jointly estimate the causal effects of multiple risk factors.

2.2 Assessment of GRAPPLE with real studies

2.2.1 Inference from both weak and strong genetic instruments under no pleiotropy

We first examine whether GRAPPLE provides reliable statistical inference combining weak and strong instruments under an artificial setting with real GWAS summary statistics. In this setting, we make X and Y be the same trait from two non-overlapping cohorts, thus $\gamma_j = \Gamma_j$ for SNPs that have the same marginal association with the trait in both two cohorts, while $\hat{\gamma}_j \neq \hat{\Gamma}_j$. Though the structural equation describing the causal effect of X on Y does not exist, the linear relationship model (2) from which we estimate β still holds with $\beta = 1$ and $\alpha_j = 0$ for these SNPs. In other words, we are not estimating a meaningful “casual” effect, but are in a special case where the true β is known, which can be used to test whether GRAPPLE provides valid inference under no pleiotropy. Specifically, we consider three traits: Body mass index (BMI), Type II diabetes (T2D) and height from the GIANT and DIAGRAM consortium where sex-specific GWAS data are available [27, 33]. The female cohort is used to get $\hat{\gamma}_j$ and the male cohort is used to get $\hat{\Gamma}_j$. As a three-sample design, the UK Biobank data for corresponding traits are used for SNP selection. The true β is 1, when we assume that all selected instruments have no gender-specific association with the traits. For benchmarking, we compare the performance of GRAPPLE with other three well-adopted MR methods, inverse-variance weighted (IVW) [10], MR-Egger [4] and weighted median [5] with the sample three-sample design.

We compare across different p-value threshold for instrument selection, ranging from a stringent threshold 10^{-8} to a mild threshold 10^{-2} (Figure 2a). GRAPPLE keeps providing unbiased estimates of β showing that including weak instruments using a proper way as in GRAPPLE would not suffer from the weak instrument bias. Surprisingly, biases exist in other three MR methods even with a stringent p-value threshold, which mostly likely is due to the power discrepancy between the GWAS data for selection and estimating γ_j . In addition, the confidence intervals does get narrower with GRAPPLE for T2D, showing the potential benefit of including weak instruments for less powerful GWAS studies. Finally, we proof that the three-sample design is necessary. As shown in Figure S1a, the two-sample design can result in biased casual effects estimation even when the instruments only include strongly associated SNPs.

2.2.2 Level of pleiotropy in SNPs with heterogeneous strengths

Next, we check whether or not the weak instruments are more vulnerable to pleiotropy, as that can be a concern for including the weak SNPs. We examine whether independent sets of SNPs provide consistent estimates of the risk factor’s causal effect. Four risk factor and disease pairs are compared, including the effect of BMI on T2D, low-density cholesterol concentrations (LDL-C) on coronary artery disease (CAD), height on smoking, and systolic blood pressure (SBP) on stroke (Figure 2b).

SNPs passing the p-value threshold 10^{-2} in the cohort for selection are divided into three groups after LD clumping: “strong” ($p_j \leq 10^{-8}$), “moderate” ($10^{-8} < p_j \leq 10^{-5}$), and “weak” ($10^{-5} < p_j \leq 10^{-2}$). The SNPs across groups are used separately to obtain group specific estimates of the causal effect β . The estimates $\hat{\beta}$ are stable across groups (Figure 2b). Though the “weaker” SNPs provide estimates with more uncertainty due to limited power, the estimates are consistent with those from the “strong” group. Using other MR methods also show some level of consistency in estimating β across different sets of instruments, but perform worse due to weak instrument bias (Figure S1b). Thus, it shows that weak instruments are in general not providing more biased estimates than strong instruments under pleiotropy, so it is beneficial to include them also as instruments, especially for less powerful GWAS data with no strongly associated SNPs. To summarize, GRAPPLE can expand the ability to evaluate causal effect of risk factors with both strong and weak genetic instruments.

2.2.3 Identify direction of causality for known causal relationships

Then, we examine the performance of GRAPPLE in identifying the causal direction with the shape of the profile likelihood. For the causal direction, we focus on the two pairs of traits with known causal relationship: BMI on T2D, and LDL-C on CAD. We switch the role of the risk factor and disease to see if the correct direction can be revealed. Specifically, we treat T2D and CAD as the “risk factor”, and BMI and LDL-C as the corresponding “disease” (Figure 2c). For T2D, the cohort for the other gender is used for SNP selection and for CAD, the risk factor cohort used is from [15] and the selection p-values are from [41]. As expected, we see that when the role of the risk factor and disease is reversed, the profile likelihood shows a main mode at 0, and a weaker mode around $1/\beta$.

2.2.4 Multiple pleiotropic pathways in the effect of C-reactive protein

Finally, we test for our ability to identify multiple pleiotropic pathways with the analysis of the C-reactive protein (CRP) effect on CAD. C-reactive protein has been found to be strongly associated with the risk of heart disease while many genes who are associated with the C-reactive protein also seem to have pleiotropic effect on lipid traits [19]. Previous MR analyses only included SNPs that are near the gene CRP to guarantee a free-of-pleiotropy analysis [14] and found that CRP has no causal effect on CAD, validated also by randomized experiments [25]. However, if the SNP selection

near CRP gene is not performed, can GRAPPLE identify the existence of multiple pathways and obtain the correct estimate of the C-reactive protein effect from its associated SNPs across the whole genome?

CRP GWAS data from [37] is used for selection and the data from [18] using a larger cohort is used for getting $\hat{\gamma}_j$. The profile likelihood shows a pattern of three modes, indicating the existence of at least three different pathways (Figure 2d). One mode is negative, one is positive and the third is around zero. The negative mode involves a few marker genes including *HNF1A* and *PVRL2*, with a marker trait LDL-C. The positive mode has marker traits pulmonary function and the C-reactive protein, and the few markers genes (*IL6R*, *ARHGAP10*, *BCL7B*, *PABPC4*) are also involved in immune response and lung cancer progression [44, 45]. The mode at 0 have marker genes *CRP* and *LEPR*, and only one marker trait the C-reactive protein.

We compare across 3 p-value thresholds (10^{-8} , 10^{-5} , 10^{-3}) and check how the existence of multiple pathways affects causal estimates of the effect of C-reactive protein in MR methods using SNPs across the genome. Including the C-reactive protein as the only risk factor, all bench-marking methods give a negative estimate of the CRP effect, which is possibly driven by bias from an LDL-C pleiotropic pathway (Figure 2e). MR-RAPS is the estimation method used in GRAPPLE only there is only one risk factor, and the three other bench-marking methods give incorrect inference of the CRP effect with a p-value of β below 0.01 for at least one SNP selection threshold (notice that the weak instrument bias is bias towards *zero* as shown in fig. 2a, thus the significance at p-value threshold 10^{-3} for MR-Egger and IVW is not due to weak instrument bias). In contrast, after using two risk factors: the C-reactive protein and LDL-C, where LDL-C is an apparent confounding risk factor from fig. 2d, the estimates of CRP effect can keep insignificant across p-value thresholds. In addition, the estimates $\hat{\beta}_{CRP}$ themselves are much closer to 0 compared with that without including LDL-C. This analysis illustrate how GRAPPLE can detect pleiotropic pathway, provide information on which confounding risk factors to adjust for, and obtain reliable inference after adjusting for additional risk factors.

2.3 A causal landscape from 5 risk factors to 25 common diseases

Finally, we apply GRAPPLE to interrogate the causal effects of 5 risk factors on 25 complex diseases through a multivariate genome-wide screen. The five risk factors are three plasma lipid traits: LDL-C, high-density lipoprotein cholesterol (HDL-C), triglycerides (TG), BMI and SBP. The diseases include heart disease, Type II diabetes, kidney disease, common psychiatric disorders, inflammatory disease and cancer (Figure 3a). Though there has been causal effects screening available across traits and risk factors [48, 36, 34], we are the first to look at the landscape of the pleiotropic pathways, which is enabled by mode detection using GRAPPLE. For each pair of the risk factor and disease, we compare across p-value thresholds from 10^{-8} to 10^{-2} . As a summary of the results, Figure 3a illustrates the average number of modes detected across the p-value thresholds for SNP selection (for modes at each p-value threshold, see Figure S2). Besides the number of modes, Figure 3a also shows the p-values for each risk factor when GRAPPLE is performed with only the single risk factor assuming the “almost random effect” model (see also Figure S2, Methods). These p-values are not valid when there are pleiotropic pathways.

Figure 3a shows that multi-modality can be detected in many risk factor and disease pairs. Multi-modality is most easily seen using the stringent p-value threshold 10^{-8} (Figure S2). However, we find that some modes are contributed by a single SNP thus is more likely an outlier than a pathway. For instance, the effect of stroke on LDL-C shows two modes when the p-value threshold is 10^{-8} or 10^{-7} (one mode around -2.3 and another mode near 0.08). However, the negative mode only has one marker SNP (rs3184504) which has been found strongly associated with hundreds of different traits according to GWAS Catalog [9] while the other mode has hundreds or marker genes. After removing the SNP rs3184504, the mode disappears. Such a mode also disappears when we increase

the p-value threshold to include more SNPs as instruments. Thus, the average number of modes serves as a strength of evidence for the existence of multiple pleiotropic pathways. Some risk factor and disease pairs show multi-modality without having a significant p-value for β , suggesting that the risk factor and disease are genetically correlated through multiple pathways but there is no evidence that risk factor has a causal effect on the disease.

We then focus on two diseases: CAD and T2D. For CAD, all five risk factors show very significant effects, though multi-modality is detected in HDL-C and SBP. First, consider the well-studied, oft-debated relationship between CAD and the lipid traits. In our results for HDL-C, with different p-value thresholds, three modes in total can show up, two being negative and one positive, indicating that the pathways from HDL-C to CAD is complicated (Figure 3b). (Figure 3b shows that one negative mode is contributed by SNPs near genes *LPL* and *BUD13*, which are strongly associated with triglycerides. Another positive mode is contributed by SNPs near genes *ALDH1A2* and *PSKH1*, which is related to respiratory diseases [50]. The markers of the other negative mode are mapped to genes including *LIPG* and *CETP*).

Since the effects of the lipid traits are generally complicated, we combine all 5 risk factors and run an MR jointly with GRAPPLE (Figure 3c) with different p-value thresholds. After adjusting for other risk factors, the two most prominent risk factors for the heart disease are LDL-C and SBP, while the protective effect of HDL-C stays negligible as well as the risk brought by TG. So these results show that HDL-C as a single measurement does not seem to have a protective effect on heart disease, while there are complicated multiple pathways involved. Researchers have suggested analyzing different subgroups of HDL-C as smaller particles tend to have a stronger protective effect [57].

Lipids are involved in a number of biological functions including energy storage, signaling, and acting as structural components of cell membranes and have been reported to be associated with various diseases [52, 21, 53, 24, 32, 1]. Besides CAD, another disease that most likely involves the lipid traits is the Type II diabetes (Figure 3a). T2D is associated with dyslipidemia (i.e., higher concentrations of TG and LDL-C, and lower concentrations of HDL-C), though the causal relationship is still unclear [20]. In the mean time, evidence has emerged that LDL-C reduction with statin therapy results in a modest increase in risk of T2D [52]. For the MR analyzing each risk factor alone, we see potential protective effects of LDL-C and HDL-C on T2D but also multi-modality patterns. Two modes shows up in the profile likelihood from HDL-C to T2D where one negative mode has a marker gene *LPL* and a mode near 0 with marker genes *CETP* and *AC012181.1*. Thus we include all 3 lipid traits, along with *BMI* and run a joint model for these 4 risk factors using GRAPPLE (Figure 3d). Our result indicates a mild protective effect of HDL-C on T2D, while showing no enough evidence for the effect of either LDL-C or TG.

3 Discussion

We propose a comprehensive framework that utilizes both strong and weakly associated SNPs to estimate the causal relationship between complex traits. GRAPPLE is robust to pervasive pleiotropy and can identify multiple pleiotropic pathways. The multivariate MR in GRAPPLE can adjust for known confounding risk factors.

GRAPPLE incorporates several improvements over existing MR methods. It gets rid of weak instrument bias by dealing with measurement errors of the SNP effects on exposure with profile likelihood, which is superior to most other methods that can not deal with weak instrument bias. Our likelihood is similar to the models in [12], but we add random effects and robustify the likelihood to make it more realistic under pervasive pleiotropy. The multi-modality visualization shares similarities with [22], which estimates the causal effect by the global mode, but we provide a more comprehensive analysis of multiple pleiotropic pathways. Some recent methods used mixture models to adjusted for

pleiotropic pathways, but only allow the existence of one pleiotropic pathway [39, 36, 11, 34]. Our causality direction identification is related to bi-directional MR [49] where if we reverse the role of risk factor and disease, the estimated causal effect is likely to be 0 as the selected IVs would likely to affect the disease through unrelated risk factors. We make this idea visible and tolerate scenarios where IVs affect the disease through risk factors are selected and would bias the conclusion in the reverse MR. Finally, as the intercept term for “directional” pleiotropy in MR-Egger is not invariant to the arbitrary assignment of effect alleles for each SNP, leading to the deficiency of the method, GRAPPLE does not include any intercept term.

GRAPPLE needs a separate GWAS cohort of the exposure for SNP selection, which is necessary for valid inference with weakly associated SNPs. Currently, we find it hard to obtain multiple good-quality public GWAS summary statistics with non-overlapping cohorts. We suggest that the stage-specific or study-specific GWAS data before meta-analysis may be released to the public in the future.

In GRAPPLE, we still require using a p-value threshold, though it can be as mild as 10^{-2} , instead of requiring no p-value threshold at all. There are two main reasons for this requirement. One consideration is to increase power, as including too many SNPs with $\gamma_j = 0$ or extremely small would instead increase the variance of $\hat{\beta}$ [56, 55]. Another consideration is that we would not want unmeasured risk factors that are unassociated (or very weakly associated) with target risk factors to bring in large pleiotropic effects on SNPs that mainly affect these unmeasured risk factors. The chance of including these SNPs would be much lower by requiring a mild p-value threshold.

Finally, when discussing the causal effect of a risk factor, one implicit assumption we use is consistency, assuming that there is a clear and only one version of intervention that can be done on the risk factor. However, interventions on risk factors such as BMI are typically vague. For instance, there can be multiple ways to change weight, such as taking exercise, switching to different diet or conducting a surgery. It is common sense that these different interventions would have different effects on diseases, though they may change BMI by the same amount. Similarly, cholesterol has abundant functions in our body and involve in multiple biological processes. Intervening different biological processes to change the concentrations of lipid traits may also have different effect on diseases. With MR, the interventions are changing risk factors levels with natural mutations, which may be different from interventions with drugs that has a rapid and strong effect on the risk factors. We think that our causal inference using GRAPPLE, along with the markers we detect, would provide abundant information to deeper our understanding of the risk factors. However, one still needs to be careful when giving causal interpretations of the results. One recommendation in practice is to triangulate the results from MR with other sources of evidence [35].

Methods

Model details

The structural equations (1) where $\mathbf{X} = (X_1, X_2, \dots, X_K)$ and $\boldsymbol{\beta} = (\beta_1, \beta_2, \dots, \beta_K)$ describe how individual level data are generalized. To link it with the GWAS summary statistics data, denote

$$\gamma_{jk} = \operatorname{argmin}_{\gamma} \operatorname{Var}[X_k - \gamma Z_j]$$

$$\alpha_j = \operatorname{argmin}_{\alpha} \operatorname{Var}[f(\mathbf{U}, \mathbf{Z}, E_Y) - \alpha Z_j]$$

Then we can rewrite the structural equations into the following linear models:

$$X_k = \gamma_{jk} Z_j + [g_k(\mathbf{U}, \mathbf{Z}, E_{X_k}) - \gamma_{jk} Z_j] = \gamma_{jk} Z_j + \epsilon_{jk} \quad (5)$$

$$Y = \mathbf{X}^T \boldsymbol{\beta} + \alpha_j Z_j + [f(\mathbf{U}, \mathbf{Z}, E_Y) - \alpha_j Z_j] = \mathbf{X}^T \boldsymbol{\beta} + \alpha_j Z_j + \tilde{e}_j \quad (6)$$

where $\text{corr}(Z_j, \epsilon_{jk}) = 0$ for any k and $\text{corr}(Z_j, \tilde{e}_j) = 0$. By replacing \mathbf{X} in (6) with (5), we get

$$Y = (\gamma_j^T \beta + \alpha_j) Z_j + \tilde{e}_j + \sum_k \beta_k \epsilon_{jk} = \Gamma_j Z_j + e_j$$

where $\Gamma_j = \gamma_j^T \beta + \alpha_j$. As $\text{Corr}(Z_j, e_j) = \text{Corr}(Z_j, \tilde{e}_j + \sum_k \beta_k \epsilon_{jk}) = 0$, we conclude that Γ_j also satisfies that

$$\Gamma_j = \text{argmin}_{\Gamma} \text{Var}[Y - \Gamma Z_j].$$

Thus, both Γ_j and γ_{jk} represent marginal associations between SNP Z_j and the traits of the disease and risk factors, and their relationships follow Equation (2).

When the disease is a binary trait, the structural equation of Y changes to

$$\text{logit}[P(Y = 1)] = \mathbf{X}^T \beta + f(\mathbf{U}, \mathbf{Z}, E_Y) \quad (7)$$

With the same argument, we have

$$\text{logit}[P(Y = 1)] = \Gamma_j Z_j + e_j$$

If we further assume that for each genetic instrument j , Z_j is actually independent of e_j , then the odds ratio that is estimated from the marginal logistic regression will be approximately Γ_j/c with a constant $c > 1$. In other words, Equation (2) is still approximately correct with the β in (2) a biased (by a ratio of $1/c$) version of the β in (7) (for a detailed calculation, see A.1 of [56]).

GWAS summary statistics from overlapping cohorts

The GWAS estimated effect sizes (log odds ratios for binary traits) of SNP j are $\hat{\Gamma}_j$ for the disease and a length K vector $\hat{\gamma}_j$ for the risk factors. As shown in [7] and derived in SI text without assuming a polygenic model [8], for any risk factor k we have

$$\text{Corr}[\hat{\Gamma}_j, \hat{\gamma}_{jk}] \approx \frac{N_{sk}}{\sqrt{N_{ek} N_o}} \text{Corr}[Y_s, X_{ks}] \quad (8)$$

where N_o and N_{ek} are the total sample sizes for the disease and k th risk factor. N_{sk} is the number of shared samples. The correlation of X_k and Y of any shared sample is $\text{Corr}[Y_s, X_{ks}]$. The standard derivation of $\hat{\Gamma}_j$ and $\hat{\gamma}_{jk}$ are denoted as σ_{Y_j} and $\sigma_{X_{jk}}$, which can be considered as known values from the GWAS summary statistics. Equation (8) shows that all the SNPs share the same correlation. As a consequence, we assume

$$\begin{pmatrix} \hat{\Gamma}_j \\ \hat{\gamma}_j \end{pmatrix} \sim \mathcal{N} \left(\begin{pmatrix} \Gamma_j \\ \gamma_j \end{pmatrix}, \begin{pmatrix} \sigma_{Y_j} & & & \\ & \sigma_{X_{j1}} & & \\ & & \ddots & \\ & & & \sigma_{X_{jK}} \end{pmatrix} \Sigma \begin{pmatrix} \sigma_{Y_j} & & & \\ & \sigma_{X_{j1}} & & \\ & & \ddots & \\ & & & \sigma_{X_{jK}} \end{pmatrix} \right) \quad (9)$$

where Σ is the unknown shared correlation matrix.

Estimate the shared correlation Σ

To estimate Σ from summary statistics, we can use equation (8). We first select unassociated SNPs where $\gamma_{jk} = 0$ for all risk factors k as the SNPs with their selection p-values $p_{jk} \geq 0.5$ for all k .

Denote their Z-values of the estimated effect sizes of both risk factors and disease as matrix $Z_{T \times (K+1)}$ where T is the number of selected unassociated SNPs. Then the estimated covariance is $Z^T Z / T$ from which we get the estimated correlation matrix.

IV selection using LD clumping

In GRAPPLE, we need to first select a set of independent SNPs as instruments. As shown in [56], the correlations of the estimates $\hat{\Gamma}_j$ and $\hat{\gamma}_j$ across independent SNPs are negligible. If the instruments are correlated, stronger assumptions are needed to account for the correlation even when the r^2 between any pair of SNPs are “known”. Thus, we only use independent SNPs as instruments to simplify the calculation. Besides the independence requirement, we only include SNPs that pass a p-value threshold. As shown in Figure S1, there is a selection bias if the SNP selection and estimates $\hat{\gamma}_j$ are obtained from the same cohorts or even cohorts with many overlapping samples.

Thus, for each risk factor, we need a separate cohort as the selection cohort that has no-overlapping samples with the risk factor and disease cohorts. If $K = 1$, the selection p-value is the reported p-values for the SNPs in the selection cohort. For multiple risk factors, the selection p-value is the Bonferroni combined p-values $K \min(p_{jk})$ across the K traits where p_{jk} is the selection p-value of SNP j and trait k . We take the intersection of the SNPs that are measured in all selection, risk factor and disease cohorts as candidate SNPs and use LD clumping with PLINK [26] to select independent SNPs whose selection p-values are smaller than some threshold. The LD r^2 threshold is set to 0.001.

Estimate the effects β

Here, we perform statistical analysis with the random effect model $\alpha_j \sim N(0, \tau^2)$ for the pleiotropic effects, while robust to outliers where the pleiotropic effects for a few instruments are large.

First, we define for each SNP j the statistics

$$t_j(\beta, \tau^2) = \frac{\hat{\Gamma}_j - \hat{\gamma}_j^T \beta}{\sqrt{\sigma_{Y_j}^2 + \beta^T \Sigma_{X_j} \beta - 2\beta^T \Sigma_{X_j Y_j} + \tau^2}} \quad (10)$$

where Σ_{X_j} is the variance of $\hat{\gamma}_j$ and $\Sigma_{X_j Y_j}$ is the covariance between $\hat{\gamma}_j$ and $\hat{\Gamma}_j$ in our model (9). Under our assumption, $t_j(\beta, \tau^2) \sim \mathcal{N}(0, 1)$ at the true value of β and τ for most SNPs. Define the robust profile likelihood as the optimization function

$$l(\beta, \tau^2) = - \sum_j l_j(\beta, \tau^2) = - \sum_j \rho(t_j(\beta, \tau^2)) \quad (11)$$

where $\rho(\cdot)$ is some loss function. By default, GRAPPLE uses the Tukey’s bi-weight loss function. We maximize the robust profile likelihood as well as solving the following estimation equation for the heterogeneity τ^2 which is

$$\varphi_2(\beta, \tau^2) = l(\beta, \tau^2) - p\delta = 0 \quad (12)$$

where $\delta = \mathbb{E}[\rho(Z)]$ with $Z \sim \mathcal{N}(0, 1)$ following a standard Gaussian distribution. The estimates $\hat{\beta}$ and $\hat{\tau}^2$ are obtained using an alternating algorithm: fixing τ^2 to estimate β by maximizing equation (11) and fixing β to estimate τ^2 as the root of Equation (12). It has been shown in our previous work [56] for $K = 1$ that these estimates are consistent and asymptotically normally distributed when the number of SNPs are large enough. The variance of $\hat{\beta}$ and $\hat{\tau}^2$ are further calculated using the delta method with second order Taylor expansions and their confidence intervals can be constructed with these variances. For further mathematical details of the estimation, see SI.

Identify pleiotropic pathways via the multi-modality diagnosis

If there is a confounding Genetic Pathway 2 \tilde{X} , as shown in Figure 1a, that are missed, then we have the structural equation

$$Y = \beta X + \kappa \tilde{X} + f(U, Z_1, \dots, Z_p, E_Y)$$

and also the linear model

$$X = \delta \tilde{X} + \epsilon, \quad \text{Corr}(Z_j, \epsilon) = 0 \quad (13)$$

for a SNP j that only associate with Genetic Pathway 2 and uncorrelate with X conditional on \tilde{X} . Similar to (5), we have

$$X = \gamma_j Z_j + \epsilon_j, \quad \tilde{X} = \tilde{\gamma} Z_j + \tilde{\epsilon}_j$$

Plug in (13), we have

$$\gamma_j = \delta \tilde{\gamma}_j$$

$$\Gamma_j = \beta \gamma_j + \kappa \tilde{\gamma}_j + \alpha_j = (\beta + \kappa/\delta) \gamma_j + \alpha_j$$

Thus, if there are enough SNPs like SNP j , they would contribute to another mode of (4) at $\beta + \kappa/\delta$.

The same argument works for identification of the causal direction. Say there is another \tilde{X} that affects Y but is uncorrelated with the risk factor X ($\delta = 0$). The existence of such \tilde{X} is common, unless X is the only heritable risk factor of Y . They would not affect GRAPPLE too much as with a mild p-value threshold on the associate with X , very few SNPs that strongly associate with \tilde{X} will be selected and GRAPPLE is robust to those outliers. However, SNPs associate with \tilde{X} can be used to identify the causal direction, as they will have $\gamma_j = 0$ with nonzero Γ_j that are considerably large. If the role of X and Y are switched, then γ_j and Γ_j are also switched. Also, as the selection is now based on the association with Y , a lot of SNPs that associate with \tilde{X} will be selected and contribute to a mode at 0, while the SNPs that affect Y through X will contribute to a mode at $1/\beta$.

Select marker SNPs and genes for each mode

GRAPPLE uses LD clumping with a stringent r^2 ($= 0.001$) threshold to guarantee independence among the genetic instruments. However, marker SNPs are not restricted to these independent instruments in order to get more biological meaningful markers. Marker SNPs are selected from a SNP set \mathcal{G} where the SNPs are selected using LD clumping with r^2 threshold 0.05.

Assume that there are M modes detected at positions $\beta_1, \beta_2, \dots, \beta_M$. Define the residual of SNP j ($j \in \mathcal{G}$) for mode m as

$$r_{jm} = t_j(\beta_m, 0)$$

where $t_j(\cdot, \cdot)$ is defined in Equation (10). SNP j is selected as a marker for mode m if $|r_{jm}| > t_1$ for any $m' \neq m$ and $|r_{jm}| \leq t_0$. By default, t_1 is set to 2 and t_0 is set to 1 which gives reasonable results in practice. When the marker SNPs are selected, GRAPPLE further map the SNPs to ENCODE genes where the marker SNPs locate and search for the traits that these SNPs are strongly associated with in GWA studies by querying HaploReg v4.1 [51] using the R package *HaploR*. The ratios $\hat{\Gamma}_j/\hat{\gamma}_j$ of the marker SNPs are also returned for reference (shown as the vertical bars in Figure 3b).

Compute replicability p-values across SNP selection thresholds

Each p-value shown in Figure 3a summarizes a vector of p-values across 7 different selection p-value thresholds ranging from 10^{-8} to 10^{-2} for each risk factor and disease pair. It reflects how replicable the significance is across SNP selection thresholds. Specifically, it is the partial conjunction p-value [2] for rejecting the null that β is non-zero for at most 2 of the selection thresholds. For a risk factor and disease pair k , let the p-values computed by using SNPs selected with the 7 thresholds p_{ks} where $s = 1, 2, \dots, 7$. Then rank them as $p_{k(1)} \leq p_{k(2)} \leq \dots \leq p_{k(7)}$, the partial conjunction p-value for the pair k is computed as $5p_{k(3)}$.

Code Availability

The R package GRAPPLE can be installed from Github at <https://github.com/jingshuw/GRAPPLE>.

Data Availability

All GWAS summary statistics that are used in the analyses of the manuscript are downloaded from public resources, where most of them are downloaded from the GWAS Catalog [9], and the websites of GWAS consortium GIANT, DIAGRAM, PGC, GLGC, and UKBiobank. A complete list of the datasets used in each analysis and where they are from is provided in Supplementary Tables 1 and 2 and Supplementary Note 2. Intermediate results for screening of 5 risk factors on 25 diseases are available at <https://www.dropbox.com/sh/myh8xgxne8fo17v/AABWJf781VrCGnqNFMLtnqIea?dl=0>.

References

- [1] A. P. Agouridis, M. Elisaf, and H. J. Milonidis. An overview of lipid abnormalities in patients with inflammatory bowel disease. *Annals of Gastroenterology: Quarterly Publication of the Hellenic Society of Gastroenterology*, 24(3):181, 2011.
- [2] Y. Benjamini and R. Heller. Screening for partial conjunction hypotheses. *Biometrics*, 64(4):1215–1222, 2008.
- [3] C. Berzuini, H. Guo, S. Burgess, and L. Bernardinelli. A bayesian approach to mendelian randomization with multiple pleiotropic variants. *Biostatistics*, 21(1):86–101, 2020.
- [4] J. Bowden, G. Davey Smith, and S. Burgess. Mendelian randomization with invalid instruments: effect estimation and bias detection through egger regression. *International journal of epidemiology*, 44(2):512–525, 2015.
- [5] J. Bowden, G. Davey Smith, P. C. Haycock, and S. Burgess. Consistent estimation in mendelian randomization with some invalid instruments using a weighted median estimator. *Genetic epidemiology*, 40(4):304–314, 2016.
- [6] E. A. Boyle, Y. I. Li, and J. K. Pritchard. An expanded view of complex traits: from polygenic to omnigenic. *Cell*, 169(7):1177–1186, 2017.
- [7] B. Bulik-Sullivan, H. K. Finucane, V. Anttila, A. Gusev, F. R. Day, P.-R. Loh, L. Duncan, J. R. Perry, N. Patterson, E. B. Robinson, et al. An atlas of genetic correlations across human diseases and traits. *Nature genetics*, 47(11):1236, 2015.
- [8] B. K. Bulik-Sullivan, P.-R. Loh, H. K. Finucane, S. Ripke, J. Yang, N. Patterson, M. J. Daly, A. L. Price, B. M. Neale, Schizophrenia Working Group of the Psychiatric Genomics Consortium, et al. Ld score regression distinguishes confounding from polygenicity in genome-wide association studies. *Nature genetics*, 47(3):291, 2015.
- [9] A. Buniello, J. A. L. MacArthur, M. Cerezo, L. W. Harris, J. Hayhurst, C. Malangone, A. McMahon, J. Morales, E. Mountjoy, E. Sollis, et al. The nhgri-ebi gwas catalog of published genome-wide association studies, targeted arrays and summary statistics 2019. *Nucleic acids research*, 47(D1):D1005–D1012, 2019.

- [10] S. Burgess, A. Butterworth, and S. G. Thompson. Mendelian randomization analysis with multiple genetic variants using summarized data. *Genetic epidemiology*, 37(7):658–665, 2013.
- [11] S. Burgess, C. N. Foley, E. Allara, J. R. Staley, and J. M. Howson. A robust and efficient method for mendelian randomization with hundreds of genetic variants. *Nature Communications*, 11(1):1–11, 2020.
- [12] S. Burgess and S. G. Thompson. Multivariable mendelian randomization: the use of pleiotropic genetic variants to estimate causal effects. *American journal of epidemiology*, 181(4):251–260, 2015.
- [13] S. Burgess, S. G. Thompson, and C. C. G. Collaboration. Avoiding bias from weak instruments in mendelian randomization studies. *International journal of epidemiology*, 40(3):755–764, 2011.
- [14] C Reactive Protein Coronary Heart Disease Genetics Collaboration et al. Association between C reactive protein and coronary heart disease: Mendelian randomization analysis based on individual participant data. *Bmj*, 342:d548, 2011.
- [15] Coronary Artery Disease (C4D) Genetics Consortium et al. A genome-wide association study in europeans and south asians identifies five new loci for coronary artery disease. *Nature genetics*, 43(4):339, 2011.
- [16] G. Davey Smith and S. Ebrahim. ‘Mendelian randomization’: can genetic epidemiology contribute to understanding environmental determinants of disease? *International journal of epidemiology*, 32(1):1–22, 2003.
- [17] G. Davey Smith and G. Hemani. Mendelian randomization: genetic anchors for causal inference in epidemiological studies. *Human molecular genetics*, 23(R1):R89–R98, 2014.
- [18] A. Dehghan, J. Dupuis, M. Barbalic, J. C. Bis, G. Eiriksdottir, C. Lu, N. Pellikka, H. Wallaschofski, J. Kettunen, P. Henneman, et al. Meta-analysis of genome-wide association studies in 80 000 subjects identifies multiple loci for c-reactive protein levelsclinical perspective. *Circulation*, 123(7):731–738, 2011.
- [19] P. Elliott, J. C. Chambers, W. Zhang, R. Clarke, J. C. Hopewell, J. F. Peden, J. Erdmann, P. Braund, J. C. Engert, D. Bennett, et al. Genetic loci associated with c-reactive protein levels and risk of coronary heart disease. *Jama*, 302(1):37–48, 2009.
- [20] T. Fall, W. Xie, W. Poon, H. Yaghootkar, R. Mägi, J. W. Knowles, V. Lyssenko, M. Weedon, T. M. Frayling, E. Ingelsson, et al. Using genetic variants to assess the relationship between circulating lipids and type 2 diabetes. *Diabetes*, page db141710, 2015.
- [21] A. C. R. Fonseca, R. Resende, C. R. Oliveira, and C. M. Pereira. Cholesterol and statins in alzheimer’s disease: current controversies. *Experimental neurology*, 223(2):282–293, 2010.
- [22] F. P. Hartwig, G. Davey Smith, and J. Bowden. Robust inference in summary data mendelian randomization via the zero modal pleiotropy assumption. *International journal of epidemiology*, 46(6):1985–1998, 2017.
- [23] G. Hemani, K. Tilling, and G. D. Smith. Orienting the causal relationship between imprecisely measured traits using gwas summary data. *PLoS genetics*, 13(11):e1007081, 2017.

- [24] J. R. Hibbeln and N. Salem Jr. Dietary polyunsaturated fatty acids and depression: when cholesterol does not satisfy. *The American journal of clinical nutrition*, 62(1):1–9, 1995.
- [25] M. V. Holmes, M. Ala-Korpela, and G. D. Smith. Mendelian randomization in cardiometabolic disease: challenges in evaluating causality. *Nature Reviews Cardiology*, 14(10):577, 2017.
- [26] International Schizophrenia Consortium, S. M. Purcell, N. R. Wray, J. L. Stone, P. M. Visscher, M. C. O’Donovan, P. F. Sullivan, P. Sklar, et al. Common polygenic variation contributes to risk of schizophrenia and bipolar disorder. *Nature*, 460(7256):748–752, 2009.
- [27] A. E. Justice, T. W. Winkler, M. F. Feitosa, M. Graff, V. A. Fisher, K. Young, L. Barata, X. Deng, J. Czajkowski, D. Hadley, et al. Genome-wide meta-analysis of 241,258 adults accounting for smoking behaviour identifies novel loci for obesity traits. *Nature communications*, 8:14977, 2017.
- [28] R. M. Krauss. Lipids and lipoproteins in patients with type 2 diabetes. *Diabetes care*, 27(6):1496–1504, 2004.
- [29] X. Liu, Y. I. Li, and J. K. Pritchard. Trans effects on gene expression can drive omnigenic inheritance. *Cell*, 177(4):1022–1034, 2019.
- [30] P.-R. Loh, G. Bhatia, A. Gusev, H. K. Finucane, B. K. Bulik-Sullivan, S. J. Pollack, T. R. de Candia, S. H. Lee, N. R. Wray, K. S. Kendler, M. C. O’Donovan, B. M. Neale, N. Patterson, A. L. Price, and S. W. G. o. t. P. G. Consortium. Contrasting genetic architectures of schizophrenia and other complex diseases using fast variance-components analysis. *Nature Genetics*, 47(12):1385–1392, 2015.
- [31] L. A. Lotta, S. J. Sharp, S. Burgess, J. R. Perry, I. D. Stewart, S. M. Willems, J. Luan, E. Ardanaz, L. Arriola, B. Balkau, et al. Association between low-density lipoprotein cholesterol-lowering genetic variants and risk of type 2 diabetes: a meta-analysis. *Jama*, 316(13):1383–1391, 2016.
- [32] M. Maes, R. Smith, A. Christophe, E. Vandoolaeghe, A. V. Gastel, H. Neels, P. Demedts, A. Wauters, and H. Meltzer. Lower serum high-density lipoprotein cholesterol (hdl-c) in major depression and in depressed men with serious suicidal attempts: relationship with immune-inflammatory markers. *Acta Psychiatrica Scandinavica*, 95(3):212–221, 1997.
- [33] A. P. Morris, B. F. Voight, T. M. Teslovich, T. Ferreira, A. V. Segre, V. Steinthorsdottir, R. J. Strawbridge, H. Khan, H. Grallert, A. Mahajan, et al. Large-scale association analysis provides insights into the genetic architecture and pathophysiology of type 2 diabetes. *Nature genetics*, 44(9):981, 2012.
- [34] J. Morrison, N. Knoblauch, J. Marcus, M. Stephens, and X. He. Mendelian randomization accounting for correlated and uncorrelated pleiotropic effects using genome-wide summary statistics. *BioRxiv*, 2019.
- [35] M. R. Munafò and G. D. Smith. Robust research needs many lines of evidence, 2018.
- [36] L. J. O’Connor and A. L. Price. Distinguishing genetic correlation from causation across 52 diseases and complex traits. *Nature genetics*, 50(12):1728–1734, 2018.

- [37] B. P. Prins, K. B. Kuchenbaecker, Y. Bao, M. Smart, D. Zabaneh, G. Fatemifar, J. Luan, N. J. Wareham, R. A. Scott, J. R. Perry, et al. Genome-wide analysis of health-related biomarkers in the uk household longitudinal study reveals novel associations. *Scientific reports*, 7(1):1–9, 2017.
- [38] S. Purcell, B. Neale, K. Todd-Brown, L. Thomas, M. A. Ferreira, D. Bender, J. Maller, P. Sklar, P. I. De Bakker, M. J. Daly, et al. Plink: a tool set for whole-genome association and population-based linkage analyses. *The American journal of human genetics*, 81(3):559–575, 2007.
- [39] G. Qi and N. Chatterjee. Mendelian randomization analysis using mixture models for robust and efficient estimation of causal effects. *Nature Communications*, 10(1):1–10, 2019.
- [40] E. Sanderson, W. Spiller, and J. Bowden. Testing and correcting for weak and pleiotropic instruments in two-sample multivariable mendelian randomisation. *bioRxiv*, 2020.
- [41] H. Schunkert, I. R. König, S. Kathiresan, M. P. Reilly, T. L. Assimes, H. Holm, M. Preuss, A. F. Stewart, M. Barbalic, C. Gieger, et al. Large-scale association analysis identifies 13 new susceptibility loci for coronary artery disease. *Nature genetics*, 43(4):333–338, 2011.
- [42] H. Shi, G. Kichaev, and B. Pasaniuc. Contrasting the genetic architecture of 30 complex traits from summary association data. *The American Journal of Human Genetics*, 99(1):139–153, 2016.
- [43] G. D. Smith, M. V. Holmes, N. M. Davies, and S. Ebrahim. Mendel’s laws, mendelian randomization and causal inference in observational data: substantive and nomenclatural issues. *European Journal of Epidemiology*, pages 1–13, 2020.
- [44] S. Spencer, S. Köstel Bal, W. Egner, H. Lango Allen, S. I. Raza, C. A. Ma, M. Gürel, Y. Zhang, G. Sun, R. A. Sabroe, et al. Loss of the interleukin-6 receptor causes immunodeficiency, atopy, and abnormal inflammatory responses. *Journal of Experimental Medicine*, 216(9):1986–1998, 2019.
- [45] J.-P. Teng, Z.-Y. Yang, Y.-M. Zhu, D. Ni, Z.-J. Zhu, and X.-Q. Li. The roles of arhgap10 in the proliferation, migration and invasion of lung cancer cells. *Oncology letters*, 14(4):4613–4618, 2017.
- [46] N. J. Timpson, C. M. Greenwood, N. Soranzo, D. J. Lawson, and J. B. Richards. Genetic architecture: the shape of the genetic contribution to human traits and disease. *Nature Reviews Genetics*, 19(2):110, 2018.
- [47] N. J. Timpson, B. G. Nordestgaard, R. M. Harbord, J. Zacho, T. M. Frayling, A. Tybjærg-Hansen, and G. D. Smith. C-reactive protein levels and body mass index: elucidating direction of causation through reciprocal mendelian randomization. *International journal of obesity*, 35(2):300–308, 2011.
- [48] M. Verbanck, C.-y. Chen, B. Neale, and R. Do. Detection of widespread horizontal pleiotropy in causal relationships inferred from mendelian randomization between complex traits and diseases. *Nature genetics*, 50(5):693–698, 2018.
- [49] K. S. Vimalaswaran, D. J. Berry, C. Lu, E. Tikkanen, S. Pilz, L. T. Hiraki, J. D. Cooper, Z. Dastani, R. Li, D. K. Houston, et al. Causal relationship between obesity and vitamin d status: bi-directional mendelian randomization analysis of multiple cohorts. *PLoS medicine*, 10(2):e1001383, 2013.

- [50] J. Wang, F. Li, H. Wei, Z.-X. Lian, R. Sun, and Z. Tian. Respiratory influenza virus infection induces intestinal immune injury via microbiota-mediated th17 cell-dependent inflammation. *Journal of Experimental Medicine*, 211(12):2397–2410, 2014.
- [51] L. D. Ward and M. Kellis. Haploreg: a resource for exploring chromatin states, conservation, and regulatory motif alterations within sets of genetically linked variants. *Nucleic acids research*, 40(D1):D930–D934, 2012.
- [52] J. White, D. I. Swerdlow, D. Preiss, Z. Fairhurst-Hunter, B. J. Keating, F. W. Asselbergs, N. Sattar, S. E. Humphries, A. D. Hingorani, and M. V. Holmes. Association of lipid fractions with risks for coronary artery disease and diabetes. *JAMA cardiology*, 1(6):692–699, 2016.
- [53] R. S. Yadav and N. K. Tiwari. Lipid integration in neurodegeneration: an overview of alzheimer’s disease. *Molecular neurobiology*, 50(1):168–176, 2014.
- [54] J. Yang, B. Benyamin, B. P. McEvoy, S. Gordon, A. K. Henders, D. R. Nyholt, P. A. Madden, A. C. Heath, N. G. Martin, G. W. Montgomery, M. E. Goddard, and P. M. Visscher. Common SNPs explain a large proportion of the heritability for human height. *Nature Genetics*, 42(7):565–569, 2010.
- [55] Q. Zhao, Y. Chen, J. Wang, and D. S. Small. Powerful three-sample genome-wide design and robust statistical inference in summary-data Mendelian randomization. *International Journal of Epidemiology*, 48(5):1478–1492, 07 2019.
- [56] Q. Zhao, J. Wang, J. Bowden, and D. S. Small. Statistical inference in two-sample summary-data mendelian randomization using robust adjusted profile score. *Annals of Statistics*, in press, 2020.
- [57] Q. Zhao, J. Wang, Z. Miao, N. Zhang, S. Hennessy, D. S. Small, and D. J. Rader. The role of lipoprotein subfractions in coronary artery disease: A mendelian randomization study. *bioRxiv*, page 691089, 2019.

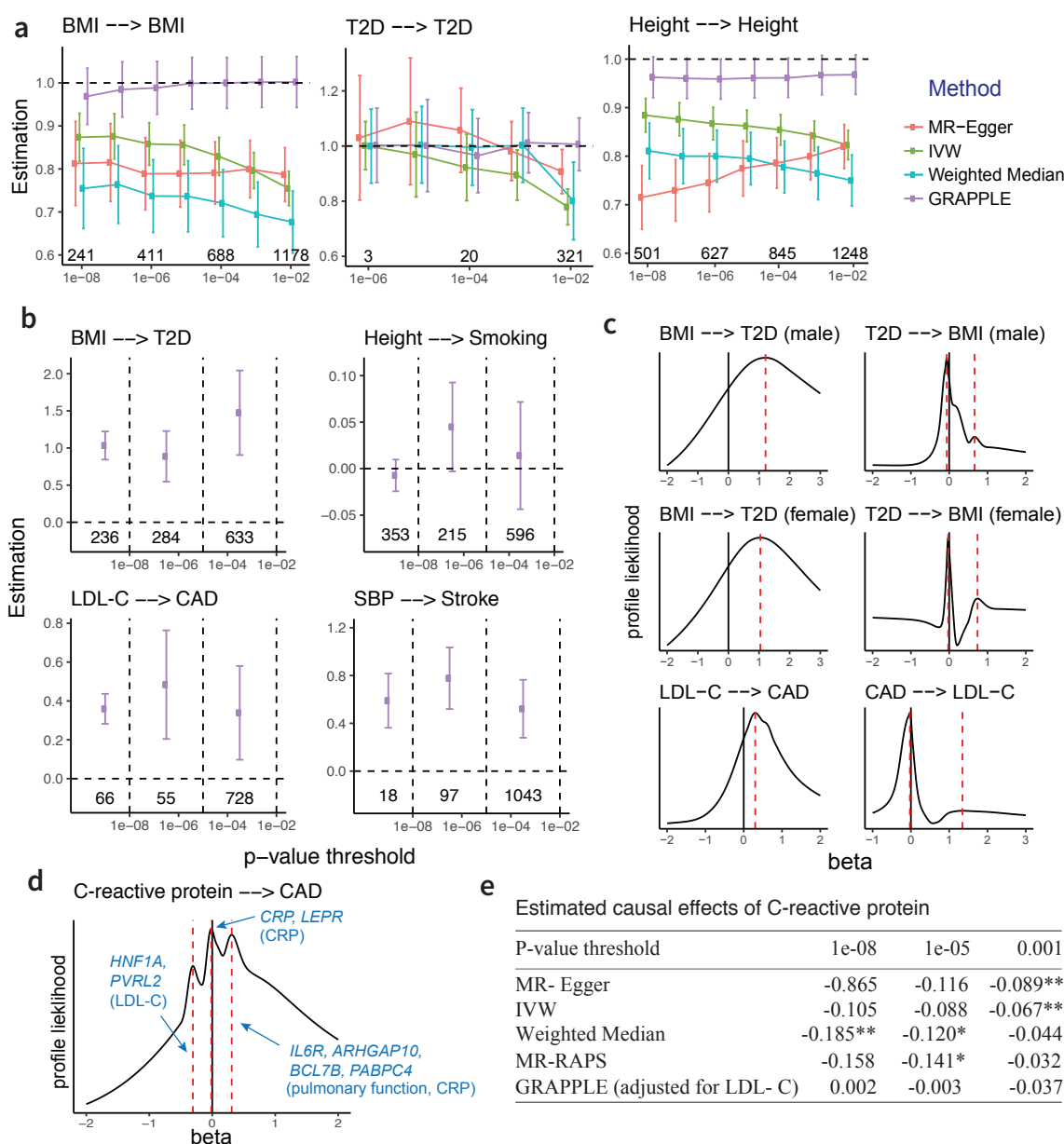


Figure 2: Evaluation of estimation accuracy of GRAPPLE. **a**, Performance of MR method across instrument selection p-value threshold under no pleiotropy. True $\beta \approx 1$ and error bars show 95% confidence intervals. The numbers are the number of independent instruments at different threshold. **b**, The estimate of β across three independent categories of SNPs with different association strengths for four risk factor and disease pairs. The numbers are the number of SNPs in each category, separated by the values of their selection p-values (dashed vertical lines). **c**, Identify causal direction by multi-modality of the profile likelihood with one mode near 0 when MR is reversely performed. The selection p-value threshold is 10^{-4} for all analyses and the red dashed lines show the positions of modes. **d**, three modes detected in the profile likelihood with selection p-value threshold 10^{-5} when analyzing the effect of CRP on CAD. Marker genes and traits (in parenthesis) are shown for each mode. **e**, estimation of CRP effect β at different p-value selection threshold for each method. The numbers are the estimated $\hat{\beta}$, with * indicating p-value below 0.05 and ** indicating p-value below 0.01.

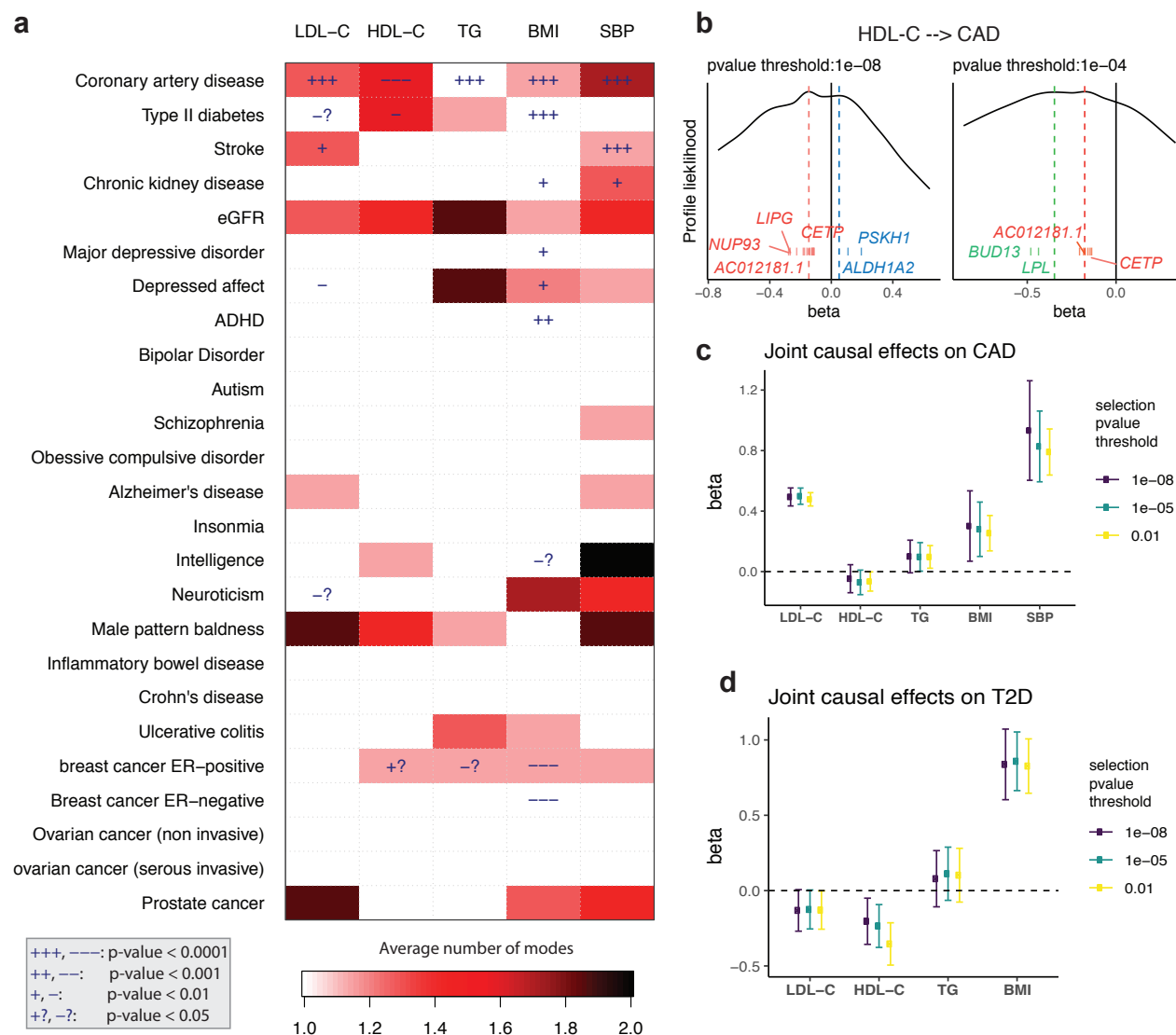


Figure 3: Screening with GRAPPLE. **a**, Landscape of pleiotropic pathways on 25 diseases. The colors show average number of modes across 7 different selection p-value thresholds. The “+” sign shows a positive estimated effect and “-” sign shows a negative estimated effect, with the p-value for each cell a combined p-value of replicability across 7 thresholds. These p-values are not multiple-testing adjusted across pairs. **b**, Multi-modality of the profile likelihood for effect of HDL-C on CAD at 2 different selection p-value threshold. Vertical bars are positions of marker SNPs ($\hat{\Gamma}_j/\hat{\gamma}_j$), labeled by their mapped genes (only unique gene names are shown). **c**, Multivariate MR with GRAPPLE for the effect of 5 risk factors on CAD. **d**, Multivariate MR with GRAPPLE for the effect of 4 risk factors on CAD. The Error bars in **c** and **d** are 95% confidence intervals.